Clays and Clay Minerals, Vol. 53, No. 4, 335–347, 2005.

CATION EXCHANGE AND PILLARING OF SMECTITES BY AQUEOUS Fe NITRATE SOLUTIONS

HAROUNA DRAMÉ*

Institute for Research in Construction, Building Envelop and Structure, National Research Council of Canada, 1200 Montreal Road, Ottawa, Canada K1A 0R6

Abstract—A comparative study of the behavior of four types of smectite is reported: two with a low Fe content, SHCa-1 (hectorite from San Bernadino, California), SWy-1 (montmorillonite from Wyoming) and two nontronites NG-1 (from Hohen Hagen, Germany) and SWa-1 (Grant County, Washington). Cation exchange was performed with a freshly prepared 1 M Fe nitrate aqueous solution. Intercalation with the same solution partially neutralized with an anhydrous carbonate solution, giving a molar ratio of $OH^-/Fe = 2$ was also studied. The modified clays were characterized by X-ray diffraction, N_2 adsorption-desorption, Mössbauer spectroscopy, thermogravimetric analysis, atomic absorption spectroscopy, X-ray fluorescence and inductively coupled plasma analysis.

In the cation exchange process, the goethite impurities grew with the Fe-rich clays but not with the Fe-poor clays. This exchange was also found to have no effect on the thermal stability and structure of the clay minerals with low Fe content, whereas it had a slight effect on the structure of the Fe-rich clays and on their thermal stability. The extent of the intercalation, however, appears to depend on the expandability of the clay layers to accommodate the Fe(III) polycations, and increases from the nontronites to montmorillonite and to hectorite. This intercalation treatment has only a slight effect on both the structure and the thermal stability of hectorite and montmorillonite. In contrast, the nontronites undergo a dramatic change in both their structure and thermal stability. The formation of Fe oxyhydroxide and oxide phases in both procedures becomes very important when the initial structural Fe content of the clay minerals is high, increasing from SHCa-1, SWy-1, SWa-1 to NG-1. The contribution of the structural Fe of the clays to the formation of the Fe oxyhydroxide is not negligible, because of partial leaching of Fe from the octahedral sheet of Fe-rich clays due to the low pH of the solutions.

Key Words—Goethite, Hectorite (SHCa-1), Hematite, Iron Exchange, Intercalation, Montmorillonite (SWy-1), Mössbauer Spectroscopy, Nontronites (NG-1, SWa-1), Pillaring, Thermal Stability.

INTRODUCTION

Cation-exchanged clays and pillared clays are two-dimensional layered materials. Exchanged clays are prepared by exchanging the natural charge-compensating cations (*e.g.* Na^+, K^+ and Ca^{2+}) on and between the swelling smectite 2:1 phyllosilicate clay layers, with a monovalent/divalent metal cation (M^{n+}) from a given metal aqueous solution. Intercalated clays are prepared by exchanging them with large inorganic hydroxy metal cations, formed by hydrolysis of metal salts. Upon heating, the hydrated metal cations or the hydroxy metal cations, respectively, undergo dehydration and dehydroxylation, forming stable dehydrated metal ions (in the exchange procedure) or metal oxide clusters (in the intercalation procedure) confined to the interlayer region of the clay. The dehydroxylated intercalated hydroxy metal cations are called pillars, and the resulting material is designated as a pillared clay. The metal oxides effectively act as pillars keeping the silicate layers separated, and create interlayer spacing (gallery spaces) of molecular dimensions, as found in zeolitic molecular sieves (Pinnavaia, 1983; Lagaly and Beneke, 1991; Gopalakrishnan, 1995; Yutaka, 1993; Maes and Vansant, 1995). In particular, the Fe(III)-exchanged clays and pillared clays have shown important potential applications as catalysts in organic synthesis and in oxidation-reduction reactions (Rightor *et al.*, 1991; Cornélis and Laszlo, 1993; Nait-Ajjou *et al.*, 1997; Chen *et al.*, 1995; Yutaka, 1993), as sorbents for the removal of heavy metal and chlorinated solvents from natural waters (McBride, 1994; Cervini-Silva *et al.*, 2000; Lenoble *et al.*, 2002; Oliveira *et al.*, 2003) and as sensors (Yutaka, 1993; Steinfink and Govea, 1994).

A comparative study is presented on the behavior of four smectites upon treatment by Fe(III) aqueous Fe nitrate solutions. The clays were SHCa-1 (hectorite from San Bernadino, California), SWy-1 (montmorillonite from Wyoming) and two nontronites NG-1 (from Hohen Hagen, Germany) and SWa-1 (Grant County, Washington). The structure of the clays is affected by the various procedures (cation exchange and intercalation) as shown by their X-ray diffraction (XRD) patterns. This study is based mainly on the characterization of Fe(III)-exchanged clays, intercalated clays, and pillared clays by PXRD (powder X-ray diffraction), BET (N_2, adsorption surface and porosity experiments), TGA/DTA

* E-mail address of corresponding author:
Harouna.Drame@nrc.ca
DOI: 10.1346/CCMN.2005.0530402

Copyright © 2005, The Clay Minerals Society

https://doi.org/10.1346/CCMN.2005.0530402 Published online by Cambridge University Press

(thermogravimetric analysis/differential thermal analysis) and ^{57}Fe Mössbauer spectroscopy.

EXPERIMENTAL METHODS

Materials

Hectorite (SHCa-1), montmorillonite (SWy-1) and two nontronites, NG-1 and SWa-1 were received as crude materials from the source clays repository of The Clay Minerals Society, University of Missouri. Clay purification procedures followed those of Villemure (1987). Quartz was removed from the hectorite and the montmorillonite samples by mechanical dispersion in distilled water followed by centrifugation (1 g of clay/100 mL distilled water). Prior to use, calcite and dolomite impurities were destroyed by treating the clay suspension with a 1 N HCl solution until the pH was reduced to 3.5 and remained at or near that value for 10 min, followed by centrifugation and washing with a solution of pH 3.5 to remove soluble salts and exchangeable basic cations. The sediment was redispersed in water, the suspension pH was adjusted to 8.0 with NaOH and allowed to stand overnight. The <0.2 μm size fraction of the clay was siphoned off from the bottom sediment and treated several times with a 1 M NaCl solution. Samples were then dialyzed for a week until the reaction with $AgNO_3$ was negative. The resulting Na^+-exchanged hectorite and montmorillonite were obtained and freeze dried. These Na^+-clays are designated NaSHCa-1 and NaSWY-1.

Since NG-1 contains large amounts of admixed Fe oxide impurities, this sample was purified by a variation of the above procedure. First, the sand fraction (70% of the sample) was removed by several sedimentations. The Fe oxide was also removed by sedimentation. The upper yellow-brown colored non-magnetic goethitic (Murad, 1987; Lear *et al*., 1988) suspension was discarded. A hand bar magnet was passed several times through the solution to remove the magnetic fraction identified as maghemite (Lear *et al*., 1988). Bright green particles of nontronite free of all previous impurities were obtained from this treatment. The magnetic phase-separation technique was not necessarily designed to remove all of the admixed magnetic phases, but the Mössbauer spectrum at room temperature of the remaining <2 μm fraction showed no sign of a magnetically ordered phase as reported elsewhere (Lear *et al*., 1988). This clay fraction was treated several times with a 1 M NaCl solution, dialyzed and then dried at 60ºC in an oven overnight. The SWa-1 nontronite was purified in the same way. However, no magnetic impurity phase was observed. These purified dried samples were designated as NaNG-1 and NaSWa-1.

Cation exchange and intercalation procedures

A weighed amount of solid $Fe(NO_3)_3.9H_2O$ was dissolved at 23ºC in 100 mL of distilled water to give a 1 M concentration of clear reddish brown ferric Fe nitrate solution (pH = 1.7).

In the cation-exchange procedure, 100 mL of this freshly prepared solution was added dropwise to 1 g of the clay material previously dispersed in 15 mL of distilled water (pH = 6.9 for hectorite and 6.4 for nontronite), under vigorous magnetic stirring at 50ºC for 24 h. The pH of the resulting slurry, formed by adding 100 mL of the ferric solution to 1 g of clay, was equal to 1.8.

There are two fundamental steps in the preparation of metal oxide-pillared clays: (1) polymeric or oligomeric hydroxy-metal cations are exchanged with the interlayer cations of the clays to give the intercalated clays; (2) the intercalated hydroxy-metal polycations are converted into oxide pillars between the silicate layers by heat treatment to give the pillared clays. Polymeric or oligomeric hydroxy-metal cations are obtained by hydrolysis of Al^{3+}, Cr^{3+} or Fe^{3+} and their complexation with anions in aqueous solution (Murad and Johnston, 1987; Murphy *et al*., 1975; Rightor *et al*., 1991; Spiro *et al*., 1966). Hydrolysis conditions such as temperature, pH, base-to-metal ratio, and period of ageing are important for the formation of the pillared clays.

In the intercalation procedure, Na carbonate solution (using anhydrous salt) was added dropwise and under vigorous magnetic stirring to the freshly prepared ferric nitrate 1 M solution to adjust the pH value of the solution, and to obtain a molar ratio of $OH^-/Fe = 2$ (Rightor *et al*., 1991; Brindley and Yamanaka, 1979; Spiro *et al*., 1996). Anhydrous Na carbonate was used as a base to prevent local high concentrations of hydroxide and the irreversible formation of a precipitate, which results when a strong base is added directly to Fe solutions. Nitrogen was bubbled through the solution to remove all dissolved CO_2 formed in the reaction. A fraction of this solution was aged for 24 h at room temperature. It was then filtered (Whatman, qualitative filter paper no. 5) to give a clear solution and to remove any precipitation products. A dark red solution of pH 1.7, free of any visible precipitate, was obtained. The other fraction was set aside for 3 months at room temperature, at the end of which a thick yellow precipitate was formed. The solution aged for 24 h was used for the intercalation studies. The supernatant liquid of the suspension aged for 3 months (3m) was used only for the intercalation of the NG-1, for comparison purposes. 100 mL of these solutions were added dropwise under vigorous magnetic stirring to the clays dispersed in 15 mL of distilled water and the reactions were performed at 50ºC for 5 h. The pH of the resulting slurry was 1.8.

The reaction in both cases (cation exchange and intercalation) was quenched by adding 200 mL of cold distilled water to the reaction media. The resulting solution was poured into a 250 mL teflon centrifuge bottle. Centrifugation and washing with distilled water (at least 7 × 250 mL) were alternated until a nitrate-free

https://doi.org/10.1346/CCMN.2005.0530402 Published online by Cambridge University Press

and clear supernatant liquid was obtained. The exchanged clays were dried overnight at 70ºC. The resulting exchanged and intercalated clays were ground and passed through a 250 mesh screen. The various Fe-exchanged clays were designated as FeSHCa-1E, FeSWy-1E, FeSWa-1E and FeNG-1E (E stands for exchanged). The color of the exchanged clays was light orange brown for hectorite and gradually a darker orange brown from SWy-1 to SWa-1 to NG-1. The intercalated clays were designated FeSHCa-1I, FeSWy-1I, FeSWa-1I and FeNG-1I (I indicates that the clay was intercalated with a solution having an OH^-/Fe molar ratio of 2). The product obtained from the solution aged for 3 months was designated FeNG-1IA (A indicates that the solution was aged for three months).

The pillared products were finally obtained by heat treatment of the intercalated clays. They were designated by adding C_T (C_T = calcination at temperature T) at the end of the abbreviation for each intercalated product. The color of the pillared products was red brown, and, as for the exchanged materials, was darker from SHCa-1 to SWy-1 to SWa-1 to NG-1.

Characterization methods

X-ray diffraction measurements were performed with a Phillips PW3710-based diffractometer using CuKα radiation. The XRD was used to ensure the effectiveness of the purification of all the materials, particularly the absence of any Fe hydroxide/oxide phases, to determine basal spacings and, finally, to characterize the products resulting from the exchanging and intercalation procedures.

Samples for XRD measurements were prepared by allowing an ultrasonic dispersion of 40 mg of the exchanged or intercalated dry clay in 2 mL of distilled water to air dry on a glass slide. The XRD patterns were recorded stepwise at 45 kV and 40 mA, with a step size of 0.02º2θ at a rate of 0.5º2θ/min from 3 to 90º2θ.

The study of the thermal stability of all the samples was conducted using TGA/DTA measurements on a Polymer Labs STA 1500H instrument with a nitrogen flow rate of 25 cc/min and a heating rate of 20ºC/min from 30 to 1000ºC.

The N_2 adsorption and desorption measurements were performed with an OMNISORP 100 analyzer. The samples were outgassed for 3 h at 300ºC at 10^{-4}–10^{-5} torr before the adsorption-desorption measurements were conducted.

Transmission ^{57}Fe Mössbauer spectra of all the calcined and uncalcined pillared clays were obtained at room temperature (RT), calibrated and folded as described elsewhere (Hargraves *et al.*, 1990) with a velocity range of ±4 mm/s or ±9 mm/s. All line positions and center shifts are given with respect to the center shift of a ^{57}Fe-enriched α-Fe absorber foil at RT. The zero velocity point on all the folded spectra also corresponds to this reference center shift.

The Fe content of all the unmodified (sodic clays) and modified (exchanged and intercalated) samples in this study was obtained by atomic absorption spectrometry (AAS). 10 mg of each sample were dissolved in a Nalgene container with 50 mL of HCl (10%) and 2 mL of HF (49%) at 60ºC overnight. The Fe content was analyzed by absorption with a 25 mA lamp and the Na content by emission. The initial Fe content and uptake after cation exchange and intercalation was also measured by X-ray fluorescence (XRF) on all the samples.

RESULTS

The XRD patterns of the different materials obtained from the cation exchange and the intercalation procedures are shown on Figure 1a–d. The patterns of the parent Na-clays for the most part indicate the absence of impurities, confirming the quality of the purification procedure. However, a negligible amount of quartz impurity remains in the case of SWy-1 at 20 and 27º2θ. They also show two major intense reflections at average angle values of 7.1º2θ and 28.6º2θ, corresponding to the 001 and 004 spacings, respectively. It is noteworthy that diluted HCl and NaOH solution treatments used during the purification did not alter the smectites. It is reported elsewhere that concentrated acid or base treatment could induce extreme leaching (McBride, 1994) or dissolution of octahedral sheets, thus altering the mineral structure (McBride, 1994; Komadel *et al.*, 1990). The XRD patterns of the purified samples show that the structural integrity is maintained (van Olphen, 1977; Villemure, 1987; Dramé, 1998). Exchanging Na-clays with 1 M aqueous Fe(III) nitrate solution causes clay-type dependent changes to the XRD patterns. From the XRD patterns of the exchanged clays (Figure 1a–d), the structure of the Fe-poor clay materials (SWy-1 and SHCa-1) is not affected. However, in the case of the Fe-rich materials (NG-1 and SWa-1), the structure is slightly affected upon exchange. The intercalation process strongly affects the structure of all the materials, as shown by the weak intensity of the 001 peak and its broadness, the disappearance of the 004 reflection, and the appearance of a new phase detected and characterized by XRD as goethite. The goethite reflections appear at 35º2θ and between 10–25º2θ and 45–65º2θ.

The XRD patterns of the Fe-rich clays are more affected than those of the Fe-poor ones. This is shown by the magnitude of the formation of the goethite phase and by the gradual disappearance of the 004 reflection from NG-1, SWa-1, SWy-1 to SHCa-1. The 004 reflection is also weakened in reverse order.

Ageing the pillaring solution for 3 months results in a change in the composition of Fe species due to the slow precipitation of growing polycations (Murad and Johnston, 1987). Figure 2 shows the effect of ageing the solution on the XRD pattern of the resulting

https://doi.org/10.1346/CCMN.2005.0530402 Published online by Cambridge University Press

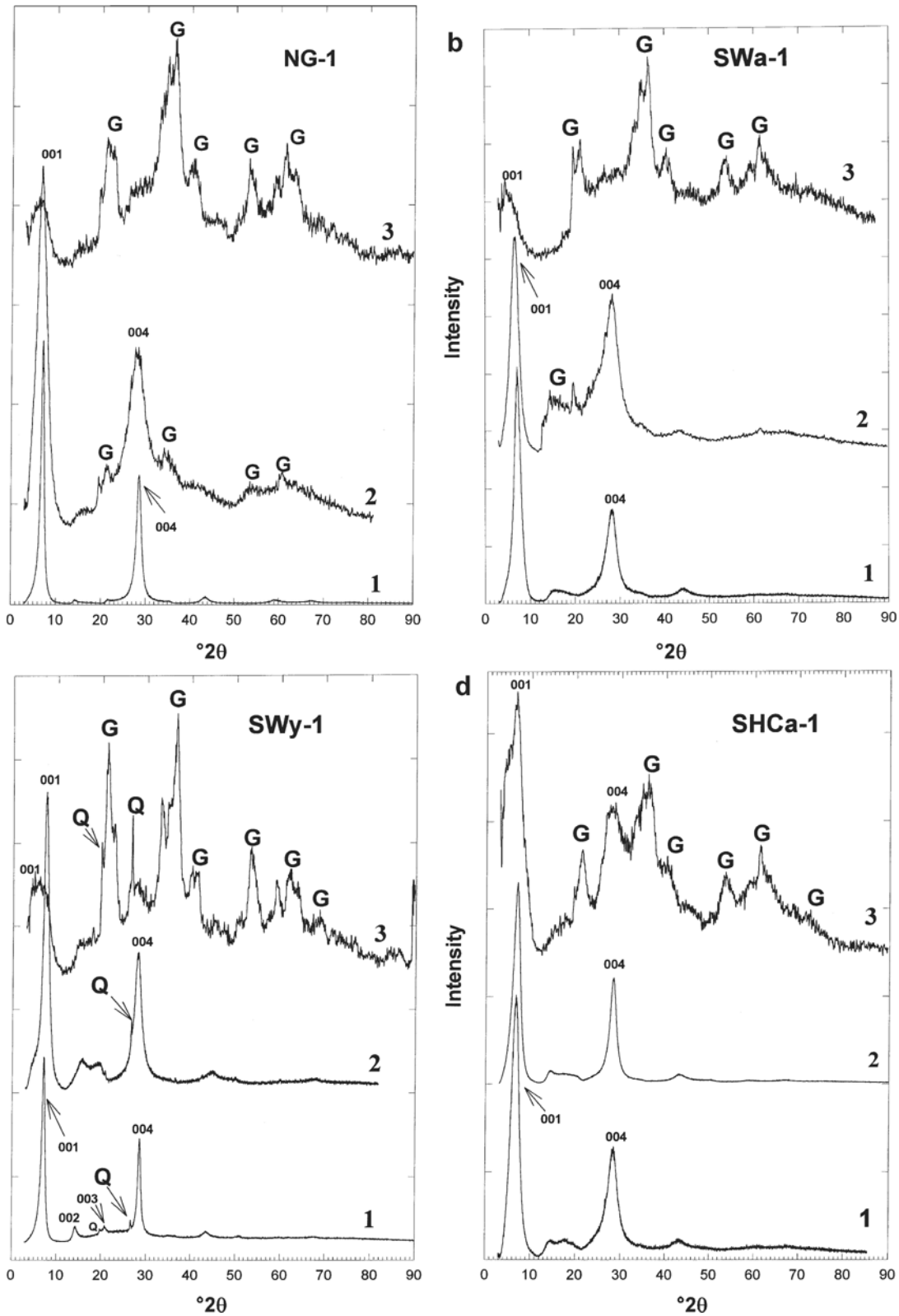


Figure 1. XRD patterns (2–90°2θ) of (a) NG-1, (b) SWa-1, (c) SWY-1 and (d) SHCa-1. In each case, three patterns are shown for the (1) sodic, (2) Fe-exchanged and (3) intercalated forms of the smectite. G = Goethite, Q = Quartz. See experimental section for more details.

https://doi.org/10.1346/CCMN.2005.0530402 Published online by Cambridge University Press

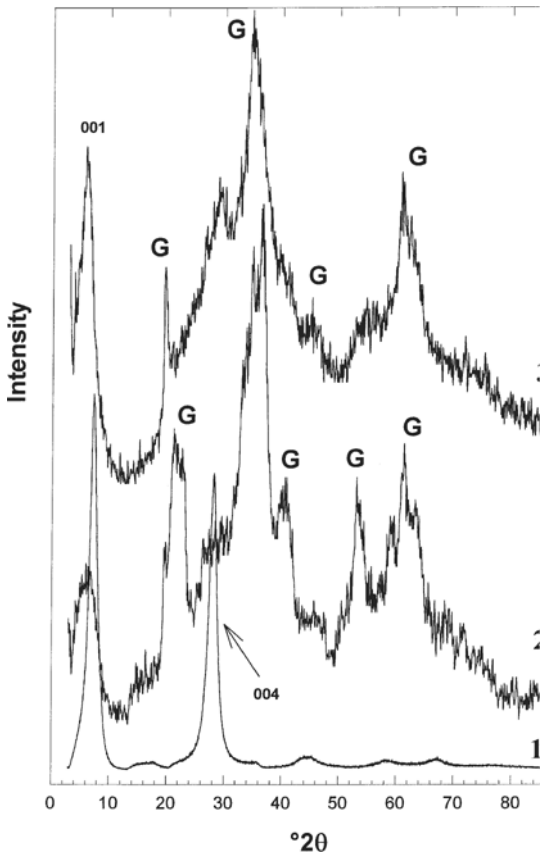


Figure 2. XRD pattern (2–90°22) showing the influence of ageing on the pillaring solution for 3 months on the structure of FeNG-1I: (1) NaNG-1, (2) FeNG-1, and (3) FeNG-1IA.

intercalated NG-1. The XRD pattern shows a narrower and more intense 001 peak, and the notable appearance of the 004 reflection which was very weak on the pattern of the intercalated NG-1 with a fresh aqueous Fe(III) nitrate solution aged for 24 h. Moreover, a noticeable reduction in the amount of the goethite phase can be observed.

The Fe contents of the various materials, as determined by AAS, are given in Table 1. The Fe content of the sodic clays is in good agreement with literature values (van Olphen and Fripiat, 1979). Upon exchange of the Na cation by Fe (III), the Fe content increases as a function of the cation exchange capacity (CEC) of the clay.

The *d* values of the basal spacing of the sodic, exchanged and intercalated clays as determined by averaging all the visible 00*l* reflections are given in Table 2. The sodic and the exchanged forms are characterized by basal spacings in a narrow range, 12.4 to 13.7 Å, corresponding to the presence of hydrated Na or Fe(III) cations in the interlamellar spaces. However, the intercalation process leads to clays characterized by basal spacings of 18.1 Å (NG-1), 19.5 Å (SWa-1), 21.6 Å (SWy-1) and 23.1 Å (SHCa-1). This is in good agreement with the intercalation of oligomeric Fe(III) species (Rightor *et al.*, 1991; Mishra *et al.*, 1996; Lenoble *et al.*, 2002).

The calcination in air at 300°C during 3 h of the sodic, exchanged and intercalated clays leads to d_{001} values reported in Table 2. In all cases, the basal spacings are reduced upon calcination. However, the basal spacings of the calcined intercalated clays, the so-called pillared clays, remain larger than that of the exchanged and sodic clays.

The specific surface area of the pillared clays and that of the parent sodic clays have been measured by the adsorption of nitrogen at 77 K. Note that the pillared clays were obtained by outgassing the intercalated clays at 300°C/3 h before performing the BET measurements. The BET surface area values are given in Table 3. The surface area is systematically increased upon pillaring, by factors from 1.4 (SWa-1) to 1.9 (NG-1), and to 2.8 (SWy-1 and SHCa-1). The increase in the specific surface due to the formation of Fe(III) oxide pillars is consistent with that reported in the literature (Yamanaka *et al.*, 1988; Mishra *et al.*, 1996; Lenoble *et al.*, 2002).

The adsorption isotherms of the sodic clays belong to type I isotherms in the Brunauer, Deming, Deming and Teller (BDDT) classification (Gregg and Sing, 1982) with a low specific surface area (Table 3). It shows a

Table 1. AAS determination of the Fe uptake by the exchanged and intercalated clays.

Sodic clays	NaNG-1	NaSWa-1	NaSWy-1	NaSHCa-1
% Fe	22.1	13.0	2.3	0.33
CEC (meq/g)	1.24	1.24	0.84	0.74
Exchanged clays	FeNG-1E	Fe-SWa-1E	FeSWy-1E	FeSHCa-1E
% Fe	26.6	17.2	3.5	2.6
	(4.5)	(4.2)	(1.3)	(2.3)
Intercalated clays	FeNG-1I	FeSWa-1I	FeSWy-1I	FeSHCa-1I
% Fe	25.2	22.4	12.0	9.1
	(3.1)	(9.4)	(9.7)	(8.7)

Percentages indicate the ratio by weight of the total amount of Fe in the different clays. The values in parentheses correspond to the percentage of the Fe(III) uptake by the sodic clays upon exchange or intercalation relative to the original Fe content of the parent Na-clays.

https://doi.org/10.1346/CCMN.2005.0530402 Published online by Cambridge University Press

Table 2. (A): d_{001} values of the uncalcined and calcined (at 300ºC/3 h) Na-clays.
(B): d_{001} values of the uncalcined and calcined (at 300ºC/3 h) Fe-exchanged clays.
(C): d_{001} values of the Fe-intercalated clays and after calcination at different temperatures.

(A)		NaNG-1	NaSWa-1	NaSWy-1	NaSHCa-1
			d_{001} (Å) values		
Dried in air (25ºC)		12.36	12.39	12.51	13.20
Calcination at 300ºC/3 h		9.58	9.68	9.68	10.17
(B)		FeNG-1E	FeSWa-1E	FeSWy-1E	FeSHCa-1E
			d_{001} (Å) values		
Dried in air (25ºC)		12.97	13.72	12.85	12.45
Calcination at 300ºC/3 h		9.85	9.96	9.78	10.75
(C)		FeNG-1I	FeSWa-1I	FeSWy-1I	FeSHCa-1I
			d_{001} (Å) values		
Dried in air (25ºC)		18.13	19.51	21.61	23.11
Calcination in air at	150 (ºC)	16.87	–	–	–
different temperatures:		(7.3)			
(pillared clays)	300 (ºC)	n.d.	13.93	14.72	15.75
			(4.4)	(5.04)	(5.6)

The values (Å) in parentheses are the height of the oxide pillar galleries.
n.d.: Undetermined d_{001} value due to near collapse of the NG-1 structure at this temperature. Calcination leads to different pillared clays.

microporous nature for the material, along with some mesoporosity as demonstrated by the presence of a narrow hysteresis loop (Gregg and Sing, 1982).The pore-size distribution (PSD) of the sodic clays was obtained by the Horvath-Kawazoe method (Horvath and Kawazoe, 1983).The PSD exhibited unimodal distribution of pores in the micropore range, and for NG-1 and of SWy-1, a shoulder extends in the mesoporous region (these data are not presented).

A typical BET adsorption isotherm of the pillared clays obtained by heat treatment of the intercalated clays at 300ºC/3 h is given in Figure 3 and the specific surface areas are indicated in Table 3. The PSD obtained is similar for each pillared clay, showing a bimodal distribution with a well developed shoulder in the mesopore range as represented in Figure 4. This result is in agreement with the presence of a type IV isotherm in all of the pillared clays (Gregg and Sing, 1982; Yamanaka *et al*., 1988; Mishra *et al*., 1996).

Both the XRD and the BET results point to the presence of Fe oxide pillars resulting from the calcination process at 300ºC. This process results in increased porosity and in the increase of the surface area of the pillared clays as reported elsewhere (Yamanaka *et al*., 1988; Yutaka, 1993; Mishra *et al*., 1996). Hence, in a comparative study between the most Fe-rich clay NG-1 and the poorest one SHCa-1, we aimed to follow up the formation of the Fe oxide upon calcination at different temperatures, and to study the behavior and the thermal stability of the corresponding pillared clays by XRD, Mössbauer spectroscopy and TGA/DTA. Figure 5 shows the XRD patterns of samples of pillared SHCa-1 and NG-1 obtained at room temperature and after heating for 3 h at 150, 300, 450 and 600ºC. The increase in temperature results in a complete loss of the 001 peak in the case of NG-1. However, for SHCa-1, this peak is still present at higher temperatures but becomes broader. The behavior of SHCa-1 upon heat treatment is similar to that reported by Yamanaka (1988) in the study of the pillaring of Na-montmorillonite by trinuclear acetate Fe nitrate solution. The splitting and the disappearance of some goethite reflections can be observed on both spectra, with the appearance of new reflections at 21, 35, 41, 53 and 63º2θ, related to the formation of Fe oxide. This Fe oxide was characterized as hematite as shown in Figure 6 by comparing the XRD reflections of the pillared NG-1 with those existing in the commercial hematite (Aldrich, 99.98%) and the calcined (at 600ºC)

Table 3. BET specific surface area (S_{BET}) measurement for sodic and pillared clays.

	Sodic clays			
	NaNG-1	NaSWa-1	NaSWy-1	NaSHCa-1
Surface area (m^2/g)	138	125	88	104
	Pillared clays			
	FeNG-1IC_{300}	FeSWa-1IC_{300}	FeSWy-1IC_{300}	FeSHCa-1IC_{300}
Surface area (m^2/g)	268	171	246	288

Pillared clays were obtained by outgassing the intercalated clays at 300ºC/3 h before performing the BET measurements.

https://doi.org/10.1346/CCMN.2005.0530402 Published online by Cambridge University Press

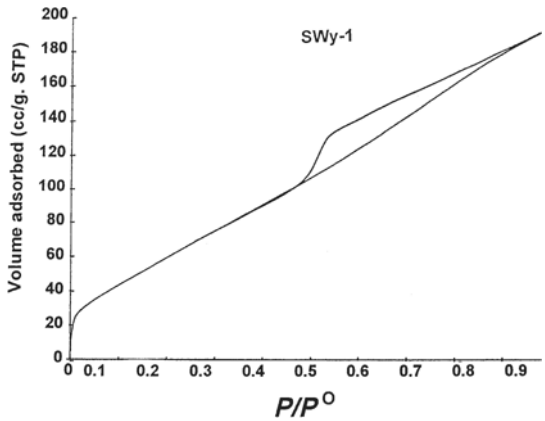


Figure 3. N_2 adsorption and desorption isotherms at 77 K of the Fe-pillared clay as a function of the relative pressure P/P_0. The adsorption isotherm of most of the Fe-pillared clays belongs to type IV in the BDDT classification. The microporous nature along with some mesoporosity are illustrated by the presence of the well opened hysteresis loop.

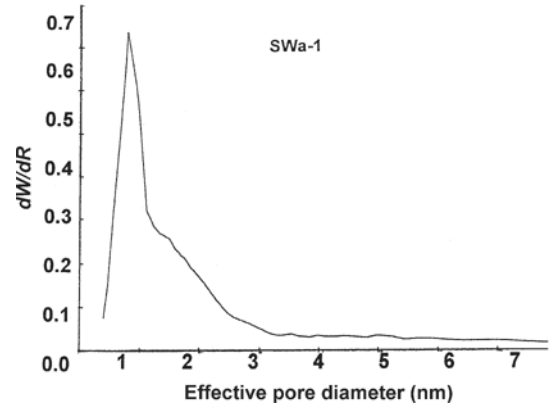


Figure 4. Typical pore size distributions of the Fe-pillared clays according to the Horvath and Kawazoe (1983) method. The pore-size distribution obtained for each pillared clay shows a bimodal distribution with a well developed shoulder in the mesopore range.

Fe oxyhydroxide precipitate (obtained from ageing the intercalating solution over 3 months). The blank experiment performed on NaNG-1 subjected to calcination at various temperatures up to 450ºC did not show any formation of Fe oxide and no behavior such as that observed for FeNG-1I.

Mössbauer spectra of the FeSHCa-1I and the FeNG-1I materials at 25ºC revealed a strong paramagnetic doublet (Goodman *et al*. 1976; Murad, 1987, 1988) with hyperfine parameter (δ = 0.35 mm/s and Δ = 0.65 mm/s) values generally consistent with Fe(III) in an octahedral site (Figures 7, 8). Whilst XRD shows the presence of a goethite phase, it could not be observed at 25ºC under our operating conditions. The observation of only one paramagnetic doublet on the intercalated clay precursor spectrum at room temperature is consistent

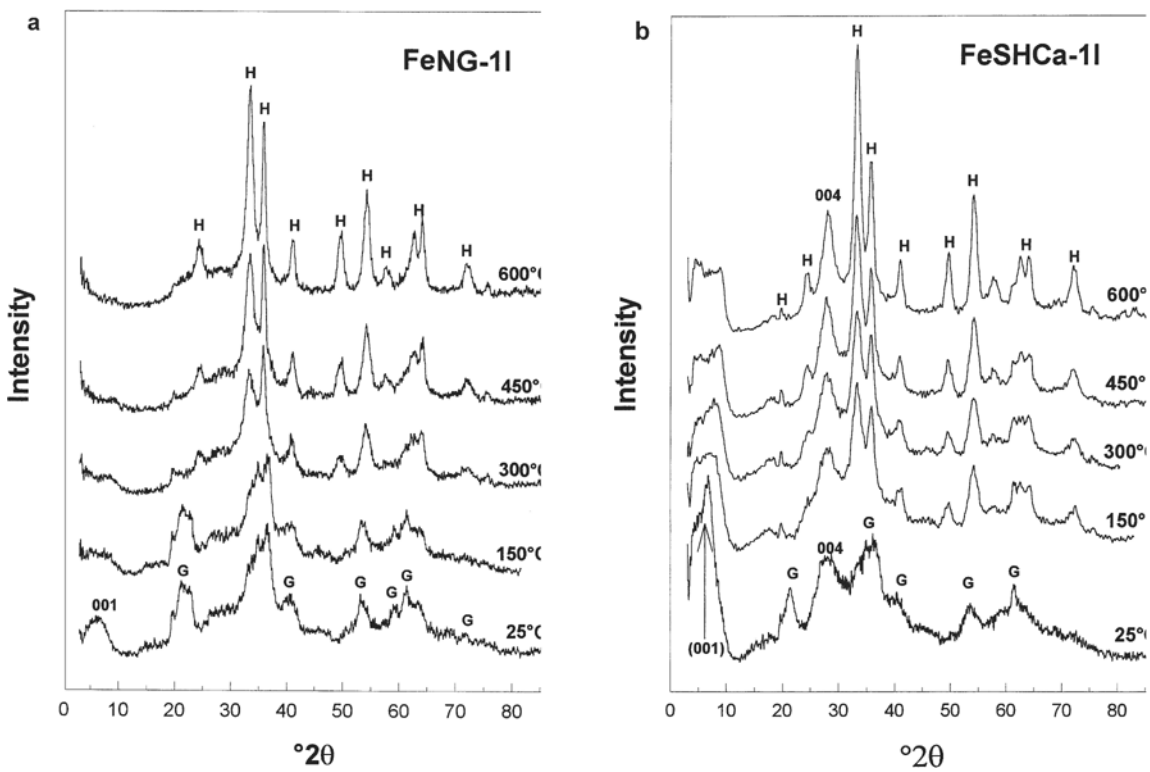


Figure 5. The comparative study of the effects of calcination temperature on the intercalated clays, FeSHCa-1I and FeNG-1I by XRD. G = goethite. H = hematite.

https://doi.org/10.1346/CCMN.2005.0530402 Published online by Cambridge University Press

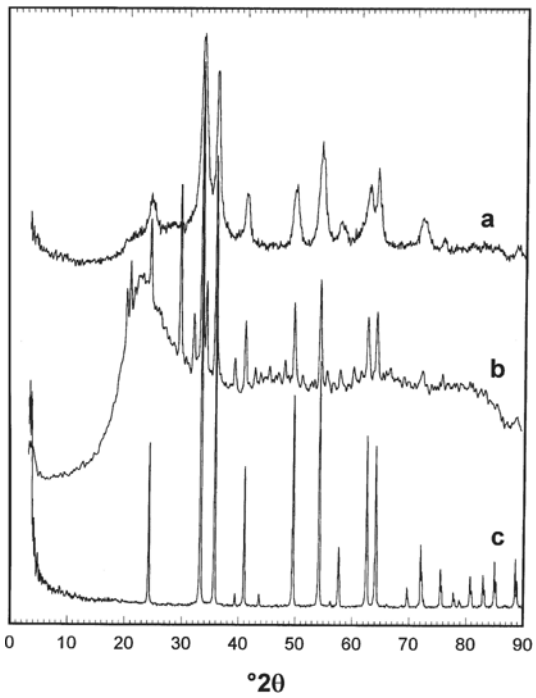


Figure 6. XRD patterns of (a) intercalated nontronite (FeNG-1I), (b) calcined (600°C/3 h) Fe precipitate from the Fe nitrate aqueous solution, and (c) commercial hematite (Aldrich, 99.98%).

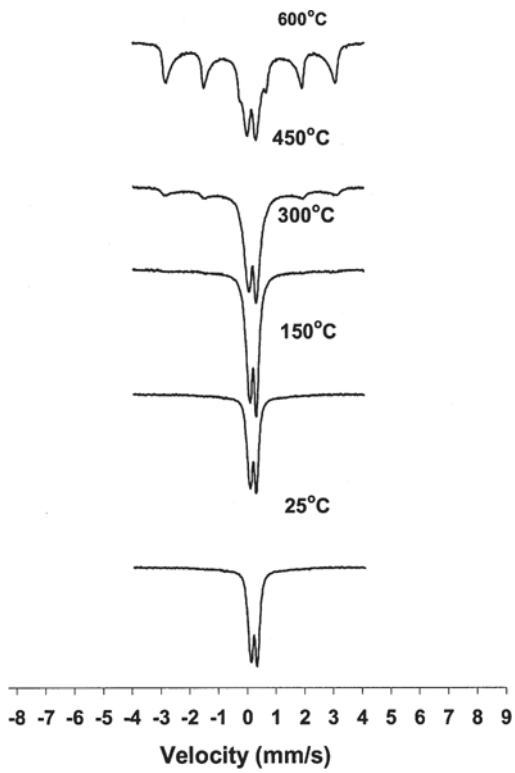


Figure 7. Mössbauer spectra recorded at room temperature (RT) for the parent intercalated FeNG-1I air-dried at 25°C and spectra for the pillared material after treatment for 3 h at 150°C, 300°C, 450°C and 600°C.

with that reported in the literature (Takada *et al*., 1964; Silver *et al*., 1980; Gangas *et al*., 1985; Doff *et al*., 1988; Bakas *et al*., 1994). The observation of one paramagnetic doublet at room temperature does not exclude the presence of a goethite phase which could be confirmed at 87 K as reported in previous studies (Murad, 1987, 1988; Lear *et al*., 1988). An increase of the calcination temperature from 25 to 600°C leads to progressive changes in the Mössbauer spectra. An additional sextet characterized by hyperfine parameters (δ = −7.95, −4.23, 0.06, 0.7, 5.13, 8.4 mm/s) corresponding to that of hematite can be clearly observed at and above 450°C in both SHCa-1 and NG-1. The XRD results (Figure 5) support the observation of formation of hematite upon calcination at higher temperatures. The hyperfine parameters of hematite are similar to those reported by other workers (Gangas *et al*., 1973, 1985; Simpoulos *et al*., 1975; Jefferson *et al*., 1975; Occelli *et al*., 1991).

The thermal stability study by TGA/DTA is shown in Figures 9 and 10. The TGA and DTA curves of the four sodic clays are shown in Figure 9a−d. The sodic clays exhibit two endothermic peaks: the first peak corresponds to the loss of physisorbed and water-solvating interlayer Na^+ cations (the minimum of the endotherm is

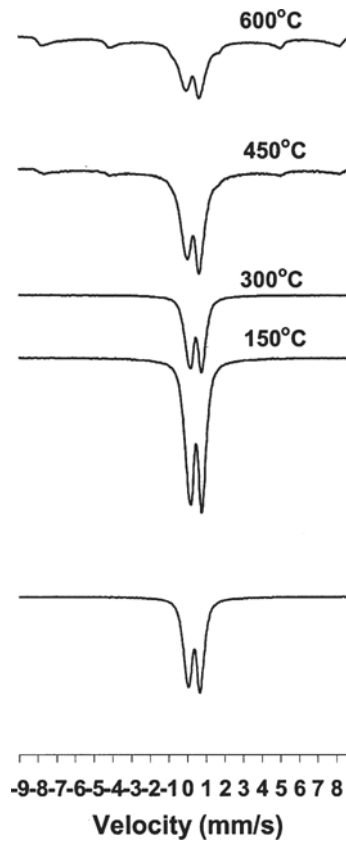


Figure 8. Mössbauer spectra recorded at room temperature (RT) for the parent intercalated air-dried clay at 25°C (FeSHCa-1I) and spectra for the pillared material after treatment for 3 h at 150°C. 300°C. 450°C and 600°C.

https://doi.org/10.1346/CCMN.2005.0530402 Published online by Cambridge University Press

at 117, 110, 105 and 111ºC, respectively, for NG-1, SWa-1, SWy-1 and SHCa-1), and the second peak corresponds to the dehydroxylation process (minimum at 439ºC for NG-1, 473ºC for SWa-1 and 700ºC for SWy-1). An ill-defined endotherm can be observed for SHCa-1 in the range 800–850ºC). In strong contrast, the intercalated clays (Figure 10a–d) are characterized by two endotherms located between 100 and 250ºC, with an exotherm situated around an average temperature of 350ºC. This exotherm is particularly pronounced for pillared NG-1. Above 350ºC, a small exotherm can be observed at 750ºC for pillared SWy-1. Similar results have been reported by other workers with pillared montmorillonite (Lenoble *et al*., 2002; Mishra *et al*., 1996). The TGA/DTA curves of the Fe-exchanged clays are not shown here but they are qualitatively similar to those of the sodic clays. The position of the second endotherm is only slightly different from that observed for the sodic clays (410ºC for FeNG-1, 436ºC for SWa-1, and 663ºC for SWy-1).

DISCUSSION

Upon cation exchange, the slight change observed in the XRD pattern for the nontronites (NG-1 and SWa-1) is probably a result of the partial leaching of the structural Fe in the octahedral sites of these clays due to the low pH of the solution. This leads to the formation of small impurities of goethite. However, no changes were observed for the other clays (SWy-1 and SHCa-1), possibly because of their low content of structural Fe (Table 1). This result is consistent with the result reported by Komadel *et al*. (1990), concerning the increased decomposition in acidic medium of clays containing Fe octahedral sheets. The Fe(III) increase is much greater for NG-1 and SWa-1 (of the order of 4%) than for SWy-1 and SHCa-1. These values correspond to the predictable values of the sodic and the exchanged clays. Interestingly, the clays are affected in accordance with their CEC values, which increases from SHCa-1 (0.74 meq/g), SWy-1 (0.84 meq/g), to SWa-1 (1.24 meq/g) and NG-1 (1.24 meq/g). Moreover, the way in which the Fe exchange affects the clays is also supported by the values of the measured relative intensities of the 001(I_{001}) and 004(I_{004}) reflections during the XRD data collection for the Na-rich clays and Fe-exchange clays (Na-rich clays/Fe-exchanged clays). The intensity ratios $((I_{001}/I_{004})_{\text{Na-rich clays}}/(I_{001}/I_{004})_{\text{Fe-exchanged clays}})$ are 15.2/10.0 (NG-1), 15.2/10.1 (Swa-1), 7.6/6.0 (Swy-1) and 7.7/8.0 (SHCa-1), respectively. This clearly demonstrated that the Fe exchange slightly affects the structure of the Fe-rich clays, whereas the Fe-poor clays remain unaffected.

In the intercalation procedure, the Fe uptake relative to the original Fe content of parent Na-clays is ~9 wt.% for SWy-1, SHCa-1 and SWa-1, but only 3.1 wt.% for NG-1. In this case, the Fe(III) uptake does not follow the CEC as seen with the Fe-exchanged clays and could be

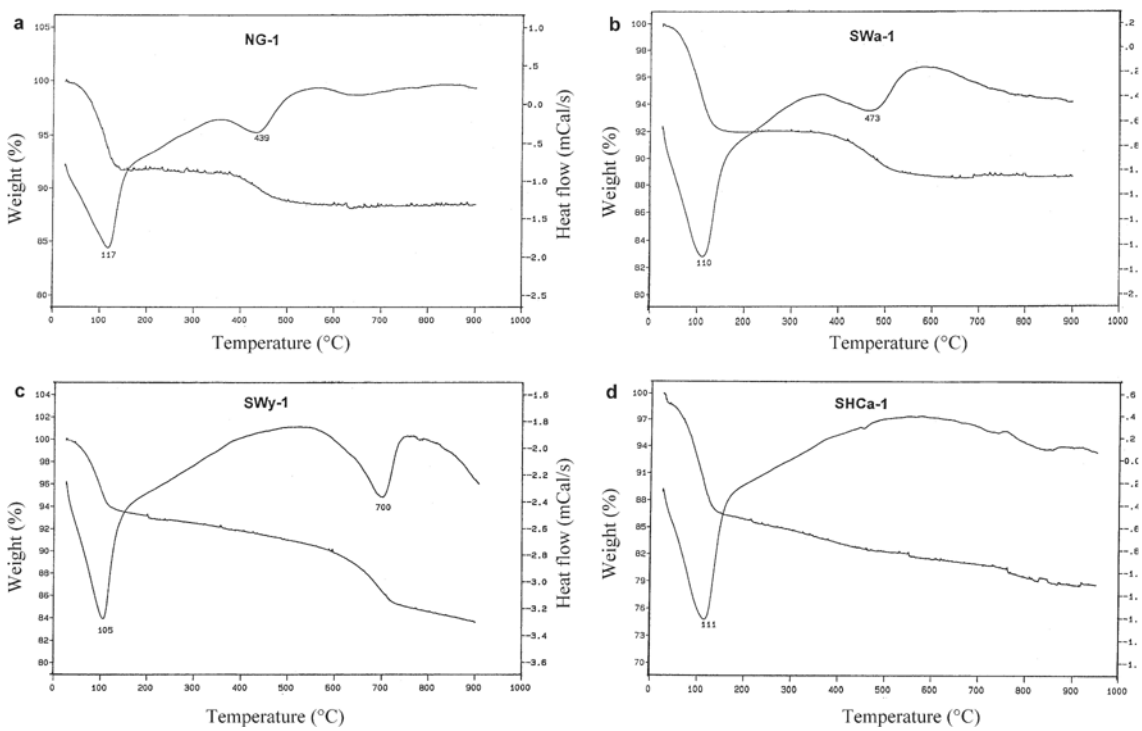


Figure 9. TG/DT analysis for the different Na-clays: (a) NaNG-1, (b) NaSWa-1, (c) NaSWy-1, (d) NaSHCa-1. The indicated temperatures are the designated endotherm (minimum) and exotherm (maximum), respectively, on the DTA curve.

https://doi.org/10.1346/CCMN.2005.0530402 Published online by Cambridge University Press

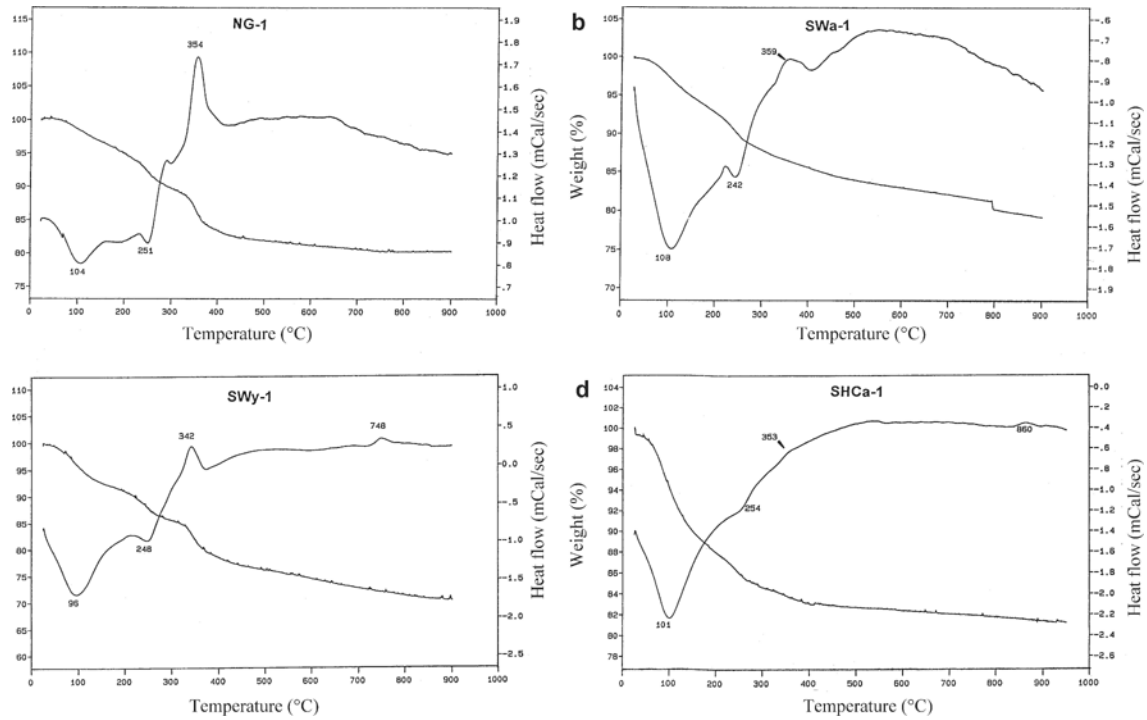


Figure 10. TG/DT analysis for the different Fe-intercalated clays: (a) FeNG-1I, (b) FeSWa-1I, (c) FeSWy-1I, and (d) FeSHCa-1I. Indicated temperatures are the designated endotherm (minimum) and exotherm (maximum), respectively, on the DT curve.

interpreted differently. First it could be related to the expandability capacity (aptitude of the clay to accommodate guest molecules within their interlamellar space) of the clays which is demonstrated by the increase of d_{001} values of the intercalated clays from NG-1, SWa-1, SWy-1 to SHCa-1 (Table 2, C). Second, it could be a consequence of the inaccessibility or clogging of some of its cation exchange sites due to the size or conformation of Fe oligomers or oxyhydroxides formed. This type of observation was found previously for a Cr acetate complex (Jimenez-Lopez *et al*., 1993). Finally, this difference in the Fe uptake may be due to the partial deformation of the clay layer because of the acid-base treatment as reported by Misra *et al*. (1996). Since the acid-base treatment affects the clay structure with the increase in Fe octahedral sheet content (Komadel *et al*., 1990), the partial deformation of Fe-rich clay layer during intercalation due to leaching of structural Fe is very likely in our case.

The weak reflection and the broadness of the 001 reflection of the intercalated clays can be attributed to some degree of interstratification as reported by Rightor *et al*. (1991). This may result from the presence in the interlamellar spaces of polycations characterized by a large distribution of sizes. The weak reflection could also result from the presence of goethite impurities due to the fact that part of the Fe(III) complex is adsorbed on the surface instead of going inside the clay layer. The composition of the intercalation solution and the presence of goethite impurities strongly affect the structure of the two nontronites as shown by their XRD patterns. This is evident from the disappearance of the 004 reflection. It results from the partial leaching of the structural Fe which leads to Fe species association (Giles *et al*., 1960; Murad *et al*., 1987) with subsequent Fe oxyhydroxide precipitation due to a change in the OH^-/Fe molar ratio of the original intercalation solution. As mentioned briefly earlier, previous results reported in the literature concerning the effect of acid and base treatments on smectites by Komadel *et al*. (1990), showed the dissolution of the octahedral sheets of smectites and the disappearance of 003 and 001 reflections upon acid treatment. The authors concluded that the intensity of the decomposition of the clay structure by the acid attack was influenced by the octahedral sheet composition and that the decomposition increased with the octahedral Fe sheets content. It is important to note that, in their operating conditions, smectites were subjected to a drastic acid and temperature treatment. Although mild treatment was used in our case, we cannot rule out the possibility that partial leaching of Fe from the octahedral sheet might have occurred for NG-1 and SWa-1, because of the low pH of the solutions. It is important to mention that the freshly prepared aqueous Fe solution, aged for 24 h and used for the intercalation, was not cloudy and did not contain any visible or filterable Fe oxyhydroxide precipitate, for at least 5 days. During the period of the intercalation procedure (5 h), however, the solution became cloudy in the case of NG-1 and SWa-1. This may be due to a

https://doi.org/10.1346/CCMN.2005.0530402 Published online by Cambridge University Press

partial leaching of the structural Fe of the clay, because of the low pH (1.8) and the resulting species association which takes place in the solution (Giles *et al*., 1960; Murad *et al*., 1987). As the Fe content of SWy-1 and SHCa-1 is very low compared to that of SWa-1 and NG-1, the leaching effect is less, and the goethite impurities are smaller. Hence, the 004 reflection in these clays is still present, but weaker. Also, the 001 reflection is less affected for SWy-1 and SHCa-1 compared to those of SWa-1 and NG-1. Two different 001 reflections were not observed in the intercalated materials, in contrast to previous reports (Rightor *et al*., 1991).

The importance of the solution composition to the structure of the intercalated clays is demonstrated by ageing, for 3 months, the partially neutralized solution of molar ratio $OH^-/Fe = 2$, allowing a change in its composition by precipitating selectively the growing polycations of different molecular weight. The reddish light brown supernatant liquid taken for the intercalation reaction contains residual polycations of lower molecular weight as demonstrated in another study (Murad *et al*., 1987). Note that ageing over 3 months leads to a complete precipitation and the supernatant liquid becomes clear with a yellow-orange precipitate deposit. The XRD spectrum of FeNG-1IA shows a sharp 001 peak, a developing 004 peak and a reduced goethite impurities reflection, in contrast to that of FeNG-1I. From these results it can be concluded that the structure is affected by the polycation composition of the intercalating solution. Moreover, the way the structure of the clays is affected depends on how strong the interaction (Ferreiro *et al*., 1995) is between the polycation species and the clay layers. Hence one can understand the origin of the delamination of the clay which was stated to be characterized by the lack of the 001 reflection in the XRD spectra, according to Rightor *et al*. (1991). Moreover, it is important to take into account the initial structural Fe content during the preparation of the intercalation solution because of its acidic pH. Otherwise, leaching or probable dissolution of the octahedral sheet could occur and lead to species association and the formation of polycations with greater size with the observed goethite surface precipitate.

While there is only a slight difference in the d_{001} values between the Fe-exchanged clays and the Na-clays, due to the difference in the respective ionic radius and/or in the interlayer cation hydration shells between Fe^{3+} and Na^+, those of the Fe-intercalated clays remained greater even upon calcination at 300ºC for 3 h (Table 2A,B,C). This result is important because it shows that a new material was created by forming Fe-oxide pillars between the clay sheets, thus propping them apart. The formation of this oxide phase results in a two-dimensional zeolite-like structure with a large specific surface area (Table 3) due to the presence of micropores and mesopores in its structure (Figure 3). These results are consistent with those reported in the literature (Rightor *et al*., 1991; Mishra *et al*., 1996; Lenoble *et al*., 2002).

The comparative study between the intercalated samples, FeNG-1I and FeSHCa-1I when subjecting them to calcination temperatures ranging from 25 to 600ºC, clearly demonstrates the instability of the Fe-rich sample compared to the Fe-poor one. The fact that no 001 reflection is observed up to 300ºC is due to the collapse of the clay interlayer space by the destruction of its structure or to increased disorder in the layer stacking. However the FeSHCa-1I sample still retains its 001 reflection up to 600ºC, demonstrating its stability over the nontronite clays (NG-1 and SWa-1). In both cases, increasing the calcination temperature leads to the formation of hematite, as shown in Figures 6–8. We have only the oxide phase for the nontronite existing at temperatures up to 300ºC, while, for the hectorite, we expect a mixed phase as the clay reflections are still present. The hematite formation takes place earlier in the nontronite sample than in the hectorite sample, which could result from the contribution of the structural Fe of the clay. This result is supported by the Mössbauer spectra obtained at 600ºC, which show a progressive build up of a strong and intense hematite magnetic sextet on the FeNG-1I spectrum (Figure 7) compared to that of the FeSHCa-1I (Figure 8). As mentioned previously, the goethite impurities formed can also contribute to the hematite formation upon heating (Goss, 1987; Ruan and Gilkes, 1995; Goodman and Lewis, 1981). Nevertheless, the contribution of goethite compared to that of the formation of the hematite phase is not significant as shown by the greater d_{001} values obtained for the intercalated clays (Table 2C). This excludes the formation of a considerable hydrous Fe oxide clay association, the formation of which would induce a slight decrease in the d_{001} basal spacing and an increase in the BET surface area as reported by Celis *et al*. (1996).

The endotherm in the DTA curve of the Fe-intercalated clays (Figure 10) located at 250ºC, following that at 100ºC (due to the removal of the physisorbed water), can be interpreted as due to the removal of the OH groups of the adsorbed goethite impurities and those formed at the surface of the clays due to the protonation of basal oxygen upon calcination. The exotherm at 350ºC, characteristic of the phase transition to hematite, is indicative of the dehydroxylation process of the polycation in the clay interlayer region and to the structural OH of the clay itself. The small exothermic peak observed in the FeSWY-1I DTA curve can be interpreted as resulting from the complete destruction of the clay structure or to a restructuring process.

A correlation of the XRD results with those obtained by TGA/DTA shows that the Fe-pillared nontronites are less stable than the Fe-pillared montmorillonite, FeSWy-1I, and the hectorite, FeSHCa-1I. The following general trend in each group corresponds to the thermal stability increase order:

https://doi.org/10.1346/CCMN.2005.0530402 Published online by Cambridge University Press

(FeNG-1I < FeSWa-1I) << FeSWy-1I < FeSHCa-1I:
Fe-intercalated clays

(FeNG-1E < FeSWa-1E) << FeSWy-1E << FeSHCa-1E:
Fe-exchanged clays

(NaNG-1 < NaSWa-1) << NaSWy-1 << NaSHCa-1:
Na-clays

The comparison between each group gives:

Fe-intercalated clays < Fe-exchanged clays < Na-clays

Intercalating these smectites by Fe(III) aqueous solution of a molar ratio $OH^-/Fe = 2$ gives a less thermally stable material compared to the materials obtained by cation exchange. In each case, the Fe-rich clays are the less stable materials. The interaction between the octahedral sheet cation and oxygen atoms determines the strength of the oxygen-hydrogen bond, which is weaker, when the neighboring cations are mostly Fe (Velde, 1992). Hence, the premature dehydroxylation of the two nontronites (NaNG-1 and NaSWa-1) compared to NaSWy-1 and NaSHCa-1 can be interpreted to be influenced by the presence of a majority of Fe^{3+} in octahedral sites. This could explain the deleterious effect of the acid-base treatment on the octahedral sheets of the clay when its Fe content increases, as found by Komadel *et al.* (1990).

The potential application of these Fe-exchanged, intercalated and pillared clays as catalysts for the hydration of styrene derivatives was reported in a previous paper (Nait-Ajjou *et al.*, 1997). Fe^{3+}-exchanged clays (SWy-1 and NG-1) were found to be active catalysts for this reaction, whereas the air-dried exchanged, intercalated and pillared clays were found inactive. Other important applications of the Fe exchange and pillared clays were mentioned in the introduction.

CONCLUSIONS

This comparative study shows that the behavior upon modification by aqueous Fe nitrate and partially neutralized ($OH^-/Fe = 2$) Fe nitrate solution of the four smectites depends on their initial structural Fe content, their CEC and on their expandability properties. Nonetheless, the octahedral and tetrahedral sheet composition might have great influence on their behavior and thermal stability.

The formation of Fe oxyhydroxide and oxide phases by both procedures becomes important when the initial structural Fe content is high, mainly in the case of NG-1 where leaching of Fe from the octahedral sheet could induce species association in solution, leading to surface precipitation of Fe oxyhydroxide. The delamination of the intercalated clays was found to depend mainly on the composition of the pillaring solution and the initial structural Fe content of the parent Na-clays.

We suggest taking into account the initial structural Fe content of the clays when preparing the intercalating solution. Otherwise, because of the low pH of the solutions, leaching of Fe from the octahedral sheet could occur and lead to the partial deformation of the clay layer or species association and the formation of polycations with greater size with the observed goethite surface precipitate.

ACKNOWLEDGMENTS

The financial support given by Natural Sciences and Engineering Research Council of Canada (NSERC) and the supervision of Dr Christian Detellier are gratefully acknowledged. The Ivory Coast government is gratefully acknowledged for a scholarship to H. Dramé. The Mössbauer spectra were recorded in the laboratory of Professor Denis Rancourt, Department of Physics (University of Ottawa) who is acknowledged for his help.

REFERENCES

Bakas, T., Moukarika, A., Papaefthymiou, V. and Lavados, A. (1994) Redox treatment of an Fe/Al pillared Montmorillonite: A Mössbauer Study. *Clays and Clay Minerals*, **42**, 634–642.

Brindley, G.W. and Yamanaka, S. (1979) A study of hydroxy-chromium montmorillonite and the form of the hydroxy-chromium polymers. *American Mineralogist*, **64**, 830–835.

Celis, R., Cornejo, J. and Hermosin, M.C. (1996) Surface fractal dimensions of synthetic clay-hydrous iron oxide associations from nitrogen adsorption isotherms and mercury porosimetry. *Clay Minerals*, **31**, 355–363.

Cervini-Silva, J., Wu, J., Stucki, J.W. and Larson, R.A. (2000) Adsorption kinetics of pentachloroethane in iron-bearing smectites. *Clays and Clay Minerals*, **48**, 132–138.

Chen, J.P., Hausladen, C.M. and Yang, R.T. (1995) Delaminated Fe_2O_3-pillared clay: Its preparation, characterization and activities for selective catalytic reduction of NO by NH_3. *Journal of Catalysis*, **151**, 135–146.

Cornélis, A. and Laszlo, P. (1993) Molding clays into efficient catalysts. *SYNLETT*, 155–161.

Doff, D.H., Gangas, J.N., Allan, M.E.J. and Coey, D.M.J. (1988) Preparation and characterization of iron oxide pillared montmorillonite. *Clay Minerals*, **23**, 367–377.

Dramé, H. (1998) Physical-chemical modifications of clay minerals: Characterization and environmental prospects as catalyst and adsorbent. PhD thesis, University of Ottawa, Canada, 343 pp.

Ferreiro, E.A., Helmy, K.A. and De Bussetti G.S. (1995) Interaction of Fe-oxyhydroxide colloidal particles with montmorillonite. *Clay Minerals*, **30**, 195–200.

Gangas, N.H., Simpoulos, A., Kostikas, A., Yassoflou, N.J. and Filippakis, S. (1973) Mössbauer studies of small particles of iron oxides in soil. *Clays and Clay Minerals*, **21**, 151–160.

Gangas, N.H., Wonterghem, V.J., Morup, S. and Koch, J.W.C. (1985) Magnetic bridging in nontronite by intercalated iron. *Journal of Physics C: Solid State Physics*, **18**, L1011–L1015.

Giles, C.H., McEwan, T.H., Nakhwa, S.N. and Smith, D.J. (1960) Studies in adsorption Part II. A system of classification of solution adsorption isotherms. *Journal of the Chemical Society*, 3973.

Goodman, B.A. and Lewis, D.G. (1981) Mössbauer spectra of aluminous goethite(α-FeOOH). *Journal of Soil Science*, **32**, 351–363.

https://doi.org/10.1346/CCMN.2005.0530402 Published online by Cambridge University Press

Goodman, B.A., Russell, J.D., Fraser, A.R. and Woodhams, F.W.D. (1976) A Mössbauer and I.R. Spectroscopy study of the structure of nontronite. *Clays and Clay Minerals*, **24**, 53–59.

Gopalakrishnan, J. (1995) Chimie douce approaches to the synthesis of metastable oxide materials. *Chemistry of Materials*, **7**, 1226–1275.

Goss, C.J. (1987) The kinetics and reaction mechanism of goethite to hematite transformation. *Mineralogical Magazine*, **51**, 437–451.

Gregg, S.J. and Sing, W.S.K. (1982) *Adsorption, Surface Area and Porosity.* Academic Press, New York.

Hargraves, P., Rancourt, D.G. and Lalonde, A.E. (1990) Single-crystal Mössbauer study of phlogopite mica. *Canadian Journal of Physics*, **60**,128–144.

Horvath, G. and Kawazoe, K. (1983) Method of the calculation of effective pore size distribution in molecular sieve carbon. *Journal of Chemical Engineering Japan*, **16**, 471–475.

Jefferson, D.A., Tricker, J.M. and Winterbottom, A.P. (1975) Electron-microscopic and Mössbauer spectroscopic studies of iron-stained kaolinite minerals. *Clays and Clay Minerals*, **23**, 355–360.

Jimenez-Lopez, A., Maza-Rodriguez, J., Olivera- Pastor, P., Maireles-Torres, P. and Rodriguez-Castellon, E. (1993) Pillared clays prepared from the reaction of chromium acetate with montmorillonite. *Clays and Clay Minerals*, **41**, 328–334.

Komadel, P., Schmidt, D., Madejová, J. and Čičel, B. (1990) Alteration of smectites by treatments with hydrochloric acid and sodium carbonate solutions. *Applied Clay Science*, **5**, 113–122.

Lagaly, G. and Beneke, K. (1991) Intercalation and exchange reactions of clay minerals and non-clay layer compounds. *Colloid & Polymer Science*, **269**, 1198–1211.

Lear, R.P., Komadel, P. and Stucki, J.W. (1988) Mössbauer spectroscopy identification of iron oxides in nontronite from Hohen Hagen, Federal Republic of Germany. *Clays and Clay Minerals*, **36**, 376–378.

Lenoble, V., Bouras, O., Deluchat, V., Serpaud, B. and Bollinger, J.C. (2002) Arsenic adsorption onto pillared clays and iron oxides. *Journal of Colloid and Interface Science*, **255**, 52–58.

Maes, N. and Vansant, E.F. (1995) Study of Fe_2O_3-pillared clays synthesized using the trinuclear Fe (III)-aceto complex as pillaring precursor. *Microporous Materials*, **4**, 43–51.

McBride, M.B. (1994) *Environmental Chemistry of Soils.* Oxford University Press, Oxford, UK, 406 pp.

Murad, E. (1987) Mössbauer spectra of nontronites: Structural implications and characterization of associated iron oxides. *Zeitschrift für Pflanzenernährung Bodenkunde*, **150**, 279–285

Murad, E. (1988) Properties and behavior of iron oxides as determined by Mössbauer spectroscopy: Pp. 309–350 in: *Iron in Soils and Clay Minerals* (J.W. Stucki, B.A. Goodman and U. Schwertmann, editors). D. Reidel, Dordrecht, The Netherlands.

Murad, E. and Johnston, H.J. (1987) Iron oxide and oxhyhydroxides. In: *Mössbauer Spectroscopy Applied to Inorganic Chemistry*, Vol. **2** (G.J. Long, editor). Plenum Publishing Corporation, New York.

Murphy, P.J., Posner, M.A. and Quick, J.P. (1975) Chemistry of Iron in Soils. Ferric hydrolysis products. *Australian Journal of Soil Research*, **13**, 189–201.

Mishra, T., Parida, K.M. and Rao, S.B. (1996) A comparative study of textural and acidic properties of Fe(III) pillared montmorillonite and pillared acid activated montmorillonite. *Journal of Colloid and Interface Science*, **183,** 176–183.

Nait-Ajjou, A., Dramé, H., Detellier, C. and Alper, H. (1997) Cation-exchanged montmorillonite catalyzed hydration of styrene derivatives. *Journal of Molecular Catalysis A: Chemical*, **126**, 55–60.

Occelli, M.L., Stencel, J.M. and Suib, S.L. (1991) Spectroscopic characterization of some iron containing pillared clays. *Journal of Molecular Catalysis*, **64**, 221-236.

Oliveira, L.C.A., Rios, R.V.R.A., Fabris, J.D., Sapag, K., Garg, V.K. and Lago, R.M. (2003) Clay-iron oxide magnetic composites for the adsorption of contaminants in water. *Applied Clay Science*, **22**, 169–177.

Pinnavaia, T.J. (1983) Intercalated clay catalysts. *Science*, **220**, 365–371.

Rightor, E.G., Ming-Shin Izou, M.S. and Pinnavaia, T.J (1991) Iron oxide pillared clay with large gallery height: synthesis and properties as a Fischer-Tropsch catalyst. *Journal of Catalysis*, **130**, 29–40.

Ruan, H.D. and Gilkes, R.J. (1995) Acid dissolution of synthetic aluminous goethite before and after transformation to hematite by heating. *Clay Minerals*, **30**, 55–65.

Simpoulos, A., Kostikas, A., Sigalas, I., Gangas, N.H. and Moukariko, A. (1975) Mössbauer study of transformations induced in clay by firing clays. *Clays and Clay Minerals*, **23**, 393–399.

Silver, J., Sweeney, M. and Morrison, L.E.G. (1980) A Mössbauer spectroscopy study of some clay minerals of the Eastern Caribbean West Indies. Part I: Spectra from 80 to 300 K. *Thermochimica Acta*, **35**, 153–167.

Spiro, T.G., Allerton, E.S., Renner, J., Terzis, A., Bils, R. and Saltman, P. (1966) The hydrolytic polymerization of iron (III). *Journal of the American Chemical Society*, **88**, 2721.

Steinfink, H. and Govea, L. (1994) Synthesis and magnetic properties of iron pillared montmorillonites. Pp. 347–357 in: *New Trends in Magnetism, Magnetic Materials, and their Applications* (J.L. Moran-Lopez and J.M. Sanchez, editors). Plenum Press, New York.

Takada, T., Kiyama, M., Bando, Y., Nakamura, T., Shiga, T., Yamamoto, N., Endoh, Y. and Takaki, H. (1964) Mössbauer study of α, β and γ-FeOOH. *Journal of the Physics Society of Japan*, **19**, 1744.

Van Olphen, H. (1977) *An Introduction to Clay and Colloid Chemistry.* John Wiley & Sons, New York.

Van Olphen, H. and Fripiat, J.J., editors (1979) *Data Handbook for Clay Materials and other Non-Metallic Minerals*. Pergamon Press, New York

Velde, B. (1992) *Introduction to Clay Minerals.* Chapman & Hall, London.

Villemure, G. (1987) Photochemical Applications of the Intercalation of Organic Cations in Clay Minerals. PhD thesis, University of Ottawa, Canada, pp. 63–65.

Yamanaka, S. and Hattori, M. (1988) Iron oxide pillared clay. *Catalysis Today*, **2**, 261–270.

Yutaka, M. (1993) Catalysis by metal ions intercalated in layer lattice silicates. *Advances in Catalysis*, **39**, 203–327.

(*Received 19 August 2004; revised 5 January 2005; Ms. 954: A.E. Peter Komadel*)

https://doi.org/10.1346/CCMN.2005.0530402 Published online by Cambridge University Press